

Document downloaded from the institutional repository of the University of Alcalá: <http://ebuah.uah.es/dspace/>

This is a postprint version of the following published document:

Varela, H., Barluenga, G. & Palomar, I. (2020) "Influence of nanoclays on flowability and rheology of SCC pastes", *Construction and Building Materials*, vol. 243, pp. 118285

Available at <http://dx.doi.org/10.1016/j.conbuildmat.2020.118285>

© 2020 Elsevier

Universidad
de Alcalá

(Article begins on next page)



This work is licensed under a

Creative Commons Attribution-NonCommercial-NoDerivatives
4.0 International License.

1 **Influence of nanoclays on flowability and rheology of SCC pastes**

2
3 Hugo Varela, Gonzalo Barluenga, Irene Palomar
4 *Department of Architecture, University of Alcala, Madrid, Spain.*

5 6 **Abstract**

7
8 SCC rheology is the key factor of fresh performance and its control is required to overcome
9 cast in place issues regarding pumping and formwork lateral pressure that still limits its
10 widespread use. Nanoclays are good candidates to improve rheological properties of cement
11 pastes as yield stress, viscosity and thixotropy, controlling paste flow behavior. However,
12 some interactions between nanoclays and admixtures can limit their efficiency. In this study,
13 a comparative analysis on rheology and flowability of SCC cement pastes blended with
14 limestone filler and 2 % by cement weight of four types of nanoclays, attapulgite, bentonite,
15 and sepiolite in powder form and dispersed in water, is presented. Two water to binder ratios
16 (w/b), 0.35 and 0.45, were considered and a high range water reducing admixture (HRWRA)
17 was used to reach the required flowability. Water adsorption of nanoclays, flowability and
18 rheological properties of SCC cement pastes with nanoclays were evaluated. It was found
19 that HRWRA was less effective on pastes with nanoclays and low w/b, particularly bentonite.
20 Sepiolite showed larger water adsorption and higher enhancing of rheological properties. It
21 was observed that, the relation of nanoclays and HRWRA was decisive to produce flowability
22 on pastes with low w/b. Besides, flowability was deeply affected by w/b, as water saturation
23 of nanoclays increased HRWRA efficiency. All nanoclays modified rheological properties
24 due to its different particles morphology characteristics, however sepiolite showed the largest
25 effects and reached the higher values of yield stress, viscosity and thixotropy ratios used.

26 **Keywords:** SCC paste; Nanoclays; water adsorption; flowability; rheology.

28 **1. Introduction**

29 Self-compacting concrete has many advantages regarding conventional concrete and has
30 gained considerable acceptance among researchers and practitioners. However, SCC presents
31 some issues regarding its cast in place that still need to be addressed, as the possible
32 rheopectic behavior when pumped and the higher formwork lateral pressure due to its large
33 flowability [1, 2]. Both issues can affect construction costs, speed and safety. Effective
34 control of rheological properties has been described to be a key factor to improve SCC cast
35 in place. For SCC pumping, a low dynamic yield stress to enhance the flowability is
36 preferred, while a static yield stress increase in time (effect of thixotropy) is necessary to
37 minimize SCC formwork lateral pressure [3].

38 Flowability and Rheology have been widely studied in cement-based materials over the last
39 decades and several testing techniques have been established. Some simple field-oriented
40 tests have been proposed to evaluate flowability parameters, as geometrical values (spread,
41 slump, height) and time values, and correlated afterwards to rheological properties as yield
42 stress and viscosity [4-10]. Jointly with this simple tests, Dynamic shear Rheometer (DSR)
43 is a rheology testing precision equipment that is used to evaluate rheological parameters, as
44 yield stress, viscosity and thixotropy, applying low shear stress or rate to material through
45 different geometries, as parallel plates, bladed vanes or coaxial cylinders [11, 12]. Coaxial
46 cylinders are a geometry used frequently on fluid cement pastes. However, the experimental
47 results depend deeply on the testing protocol applied and the geometry used [12, 13].

48 Yield stress and viscosity parameters can be obtained according to modified Bingham model
49 with a DSR controlled shear stress protocol (CS) using the rheometer software to calculate.
50 According to the literature, modified Bingham model can explain better the non-linear
51 behavior of cement pastes than other models as Bingham and Hershel-Buckley models [12,

52 14]. On the other hand, there are many methods to evaluate thixotropy parameters on SCC,
53 as *structural break down area, breakdown percentage, drop in apparent viscosity and yield*
54 *value at rest*. [15-18]. Nevertheless, a DSR protocol commonly used to evaluate thixotropy
55 parameters on pastes is the constant controlled shear rate protocol (CCR) and different
56 calculation procedures have been proposed [19-22]. Roussel proposed the flocculation rate
57 or yield stress rate growth (A_{thix}) as a parameter to evaluate the effective thixotropy of paste
58 samples at rest during a certain period of time [19, 23], while Qian proposed a thixotropy
59 index (I_{thix}) to evaluate thixotropy as the ratio between the peak yield stress and the steady-
60 state equilibrium value [3, 24].

61 A promising alternative for improving flowability and rheology is the use of
62 nanocomponents. Among them, nanoclays such as sepiolite, attapulgite, and montmorillonite
63 can modify the rheological properties of fresh concrete. These nanoclays have different
64 morphology and nature, but similar size or BET surface area [25-27]. Tregger and
65 Kawashima have demonstrated that low amounts of Attapulgite remarkably modified yield
66 stress and viscosity of cement pastes [13, 28-31]. Besides, Quanji et al. [32] showed that
67 thixotropy of cement paste increased with time and nanoclays contributed to increase this
68 effect. Ferron and Fuente explained that sepiolites can improve the stability of cement flocs
69 [33]. Kaci et al. studied the effect of bentonite on the rheological behavior of mortars and
70 found that bentonite increased yield stress after shear and reduced the characteristic time for
71 yield stress recovery [34]. Besides, some authors had showed that bentonites produce a
72 formation of house-of-card microstructure when the paste is kept at rest which may cause a
73 reduction of flowability [3, 35, 36].

74 Another point to be considered is the interaction between nanoclays, water and
75 superplasticizers (High range water reducing admixtures- HRWRA) and other polymeric

76 admixtures [37]. Nanoclays showed more affinity with water and superplasticizers than
77 cement particles because nanoclays have a S_{BET} 17 times larger than cement [38]. In fact,
78 with low amounts of nanoclays by cement weight it is possible change the consistency of
79 cement paste, mortar or concrete. Besides, the high water adsorption showed by nanoclays
80 produces a workability reduction and a viscosity increase [35, 36, 39]. Also, nanoclays are
81 able to adsorb 3-4 times of HRWRA than cement particles [38], but this adsorption varies
82 according to the type of nanoclay and the amount of water on the mixture. Moreover,
83 nanoclays combined with superplasticizers enhance thixotropy, increasing the difference
84 between the peak yield stress value and the steady-state equilibrium value [3]. Accordingly,
85 nanoclays' particle size and shape are responsible of modifying rheological properties of SCC
86 pastes [10].

87 The aim of this study was to evaluate and to characterize the influence of four different
88 nanoclays on flowability and rheology of limestone filler-cement blended pastes with two
89 w/b and different amounts of a high range water reducing admixture (HRWRA). Water
90 adsorption test, mini-cone slump test and dynamic shear rheometer test were used to provide
91 a wide comparison of nanoclays effects on cement paste fresh state. Understanding the effects
92 of nanoclays on fresh state rheological properties, as yield stress, viscosity and thixotropy,
93 would help to control SCC cement paste flow behavior. The paper presents these effects on
94 cement paste in order to overcome the issues identified on SCC in the next steps of the study.

95 **2. Experimental program:**

96 **2.1. Material and mix design**

97 The components of the pastes designed for this study are summarized in *Table 1*. A reference
98 paste with a Portland cement type I 42.5 R blended with a limestone filler, supplied by Omya

99 Clariana SL, in a ratio 2:1 was designed. Two water to binder ratios (w/b), 0.35 and 0.45,
100 were considered. In order to reach a large paste fluidity, a polycarboxylate based high range
101 water reducing admixture (HRWRA) supplied by BASF construction chemicals Spain SL
102 was used. The amount of HRWRA varied from 0 to 2% by cement weight, depending on the
103 amount required to reach the target spread. Then, 2% by cement weight of four nanoclays
104 supplied by TOLSA S.A. Group were added: attapulgite (*Att*), bentonite (*Be*) and two
105 sepiolites, one in powder form (*Sep*) and the other dispersed in water (*Sew*). Attapulgite (or
106 palygorskite) and Sepiolite are the same hydrated aluminum silicate mineral with the same
107 needle particle shape, although sepiolite has a larger particle length and BET surface area
108 (S_{BET}) [25, 26]. In contrast, Bentonite (Montmorillonite) is a smectite mineral clay with a
109 plate particle shape but with similar S_{BET} than Attapulgite [25, 27]. *Table 2* presents the main
110 particle characteristics of the nanoclays provided by the manufacturers.

111 **2.2 Experimental methods**

112 **2.2.1. Water adsorption of nanoclays: Tea-bag test**

113 The tea-bag test was carried out to evaluate water adsorption of nanoclays according to the
114 literature [37]. A tea-bag was filled with 0.3 g of nanoclay and was submerged in water. The
115 bag was weighted in wet conditions at times 0 - 180 minutes and water adsorption (*Ad*) of
116 nanoclays over time was calculated according to (*Eq. 1*) [37].

$$117 \quad Ad = \frac{(m_2 - m_1)}{m_0} \quad (\text{Eq. 1})$$

118 Where m_1 is the tea-bag wet weight at 0 minutes, m_2 is tea-bag wet weight at time t, m_0 is the
119 weight of the dry clay sample.

120 Two different pH water solutions were considered: tap water (pH - 6) and a cement pore
121 solution prepared with ordinary Portland cement and water with a 4:3 water to cement ratio
122 (pH - 11).

123 **2.2.2. Paste Flowability: Mini-cone slump test**

124 A mini-cone with dimensions 100 x 70 x 50 mm was used to evaluate cement paste spread
125 diameter, final slump and final spread flow time. A transparent methacrylate plastic base was
126 used to videotape the spread process from below. Spread diameter has been related in the
127 literature to yield stress while final spread time has been associated to paste viscosity [4-6].
128 The mini-cone test was used to evaluate the effect of water on pastes spread with nanoclays
129 and, afterwards, the effect of a HRWRA on flowability parameters of pastes with nanoclays
130 and 0.35 and 0.45 w/b ratio. The combination of both sets of results were then used to
131 evaluate the interactions among nanoclays, water and HRWRA on cement paste flowability.

132 **2.2.3. Rheological parameters: Dynamic shear rheometer (DSR)**

133 Dynamic shear rheometer test (DSR) was carried out to evaluate yield stress, viscosity and
134 thixotropy of fluid cement pastes with nanoclays. A modular rheometer (THERMO-HAAKE
135 MARS Rheostress 600) with a coaxial cylinders bob-cup geometry (CC20TiSe) was used.
136 The cup radius is 27mm, and the bob radius and height are 20mm and 34.5mm, respectively.
137 All samples were tested using a universal temperature controller (UTC) and a cryostat set at
138 25 ± 1 °C of temperature.

139 DSR test started 10 minutes after water was incorporated to the paste in the mixing process.
140 Two testing protocols were applied in this study, summarized in *Figure 1*. The first testing
141 protocol was a flow curve or controlled stress protocol (CS) that consisted in an upward ramp
142 from 10 to 1500 Pa in 300 seconds. Yield stress and viscosity were calculated using a

143 modified Bingham model [14]. The second protocol started afterwards and consisted on a
144 time curve or constant controlled rate protocol (CCR), to evaluate structural build-up and
145 thixotropy index of pastes with nanoclays. CCR procedure consisted on: a) low constant rate
146 of 0.2 s^{-1} for 30 seconds; b) high constant rate of 70 s^{-1} for 15 seconds; c) a stop (zero point)
147 for 1 second to avoid data-acquisition errors and d) low constant rate of 0.2 s^{-1} for 400 seconds.
148 According to the literature, CS protocol comprised 200 data points, while 100 data points
149 were recorded in each stage of CCR protocol [12].

150 **3. Experimental results:**

151 **3.1. Water related results**

152 **3.1.1 Water adsorption of nanoclays**

153 The experimental results of nanoclays water adsorption between 0 and 30 minutes in two
154 water solutions with different pH are reported in *Figure 2*. Water adsorption was measured
155 for 180 minutes, although all nanoclays showed a constant value before 30 minutes. All
156 nanoclays showed higher water adsorption values in cement pore solution (Alkaline pH - 11
157 solution) than in tap water. Dry nanoclays may adsorb different amount of water according
158 to morphology, nature, size or BET surface area [36, 39]. The highest adsorption in alkaline
159 solution was measured for *Sew* (sepiolite dispersed in water), although it must be considered
160 that the measurement was done on a sample previously dried, grounded and sieved, to obtain
161 a homogeneous sepiolite powder, and re-watered afterwards. *Att* was the nanoclay with lower
162 adsorption, around half of *Sew* value. On the other hand, all nanoclays showed a similar water
163 adsorption value in tap water.

164 **3.1.2. Flowability of pastes with nanoclays and different w/b.**

165 Results of mini-cone slump test of cement pastes with nanoclays and different w/b are
166 summarized in *Figure 3*. Final spread diameter (*Figure 3a*) and final spread flow time (*Figure*
167 *3b*) are plotted. Final spread diameter of the reference paste was the largest for each w/b, as
168 the incorporation of nanoclays required larger amounts of water to reach the same spread
169 diameter values than reference mixture. Paste with sepiolite in powder form (SEP) showed
170 the largest water demand to achieve the same final diameter as the pastes with the other
171 nanoclays. At 0.35 w/b, none of the pastes had started to spread, showing a dry consistency.
172 However at 0.45 w/b, REF, ATT, BE and SEW had reached around 180 mm of final spread
173 diameter while SEP had not started to spread yet. Regarding final spread flow times (*Figure*
174 *3b*) all the samples showed very short values regardless the type of nanoclay and the w/b.
175 Hence, nanoclays by themselves did not change the spread mechanism related to viscosity of
176 reference cement paste.

177 **3.2. Flowability of pastes with nanoclays and HRWRA**

178 The mini-cone slump test was also used to evaluate the effect of HRWRA on flowability of
179 cement pastes with nanoclays. This field-oriented test are useful for correlate final spread
180 diameter and final spread flow time with the rheological parameters as yield stress and
181 viscosity [4-10]. Two w/b were considered: 0.35 and 0.45. *Figure 4 and Figure 5* presents
182 the final spread diameter and final spread flow time values of pastes with nanoclays and
183 different percentages of HRWRA, for w/b of 0.35 and 0.45 respectively. It can be observed
184 that the effect of HRWRA depended strongly on w/b. While for 0.35 w/b (*Figure 4*) the
185 different type of nanoclay showed changes on HRWRA effectiveness, these differences were
186 drastically reduced for 0.45 w/b (*Figure 5*).

187 In the case of pastes with 0.35 w/b, final spread diameter and spread flow time for the same
188 amount of HRWRA were larger for reference and ATT pastes, followed by both sepiolites
189 and, at last, by BE. To achieve a fluidity of 330 ± 30 mm required for a SCC paste, reference
190 and ATT needed around 0.5 % of HRWRA while sepiolites needed 1 % and BE 1.5 %. On
191 the other hand, the final spread flow time values measured for pastes with 330 ± 30 mm final
192 diameter were similar for all pastes with values around 15 seconds.

193 When w/b ratio was raised to 0.45 (Figure 5), all pastes with nanoclays required 0.4-0.6 %
194 of HRWRA to reach 330 ± 30 mm final diameter, with final spread flow time values around
195 10 seconds. This increase of w/b improved HRWRA effectiveness reducing viscosity.

196 **3.3. Rheology evaluation of fluid cement pastes with nanoclays.**

197 Two protocols were considered to evaluate rheological properties of fluid cement paste with
198 nanoclays: controlled stress protocol (CS) and a constant controlled rate protocol (CCR)
199 (Figure 1). The CS protocol was used to evaluate yield stress and viscosity and a CCR
200 protocol was used to evaluate structural build-up. To carry out this test, only mixtures with a
201 mini-cone final spread diameter of 330 ± 30 mm were considered.

202 **3.3.1. Yield stress and viscosity**

203 *Figure 6* plots the rheology curves of fluid cement paste with nanoclays and two w/b ratio
204 (0.35 and 0.45) obtained with CS protocol and analyzed through the rheometer software. A
205 Bingham modified model was used to calculate the rheological parameters of yield stress and
206 viscosity, as the quadratic approximation produced the best adjustment in these flow curves
207 [12, 14]. Others models were used as Bingham, Herschel–Bulkley, ect. However the results
208 obtained were not robust. The yield stress and viscosity obtained with CS protocol are
209 summarized in *Table 3*. The shear stress limit value of the CS protocol of 1500Pa was not

210 reached with these pastes. The obtained flow curves (figure 6) showed maximum values of
211 shear stress down to 500 Pa due to these pastes reached first the shear rate limit value of the
212 rheometer (around 600 s^{-1}) because of the flow consistency of these pastes.

213 Pastes with nanoclays and 0.35 w/b (*Figure 6a*) had yield stress values that ranged from 8.3
214 to 94.8 Pa and viscosity from 0.29 and 0.95 Pa·s. Among them, SEW showed the highest
215 yield stress (94.8 Pa) and viscosity values (0.95 Pa·s). SEP and ATT exhibited similar yield
216 stress values (28.9 and 23.9 Pa, respectively) but SEP presented higher viscosity (0.65 Pa·s)
217 than ATT (0.46 Pa·s). BE and reference pastes had practically the same yield stress (10.0 and
218 8.3 Pa), although REF showed a viscosity (0.57 Pa·s) similar to ATT.

219 For pastes with 0.45 w/b (*Figure 6b*), yield stress values ranged from 10.6 to 48.2 Pa and
220 viscosity from 0.06 and 0.34 Pa·s. SEW showed again the highest yield stress, although it
221 was half of the value of SEW pastes with 0.35 w/b. BE was the only paste with nanoclays
222 that increased yield stress regarding 0.35, while the other pastes reduced yield stress with the
223 increase of w/b. Yield stress of the reference paste (REF) remained very similar for both w/b.
224 Besides, all pastes presented a sharp reduction of viscosity.

225 **3.3.2. Structural build up evaluation**

226 Structural build-up process was evaluated using the constant controlled shear rate protocol
227 (CCR). In this study, two parameters described in the literature were calculated: thixotropic
228 Index (I_{thix}) and the rate of reversible structural build-up (A_{thix}). Structural build-up process
229 was measured with a low constant shear rate of 0.2 s^{-1} after a pre-shear of 70 s^{-1} . Figure 7
230 plots the curves showed by the pastes with 0.35 w/b tested at 0 and 30 minutes (10 and 40
231 minutes after mixing of water, respectively) and the pastes with 0.45 w/b at 0 minutes (10

232 minutes after mixing water). All curves showed an initial peak value followed by a decline
233 until reaching a steady-state value.

234 **3.3.2.1. Thixotropy index (I_{thix})**

235 Thixotropy Index (I_{thix}) was calculated from the CCR protocol results (Figure 7) according
236 to (Eq. 2) [3, 24]:

$$237 \quad I_{thix} = \frac{\tau_i}{\tau_e} \quad (\text{Eq. 2})$$

238 where τ_i is the peak value and τ_e is the steady-state equilibrium value. I_{thix} is related to the
239 instantaneous structural break down and describes a relation between dynamic and static
240 yield stress in that point.

241 I_{thix} was calculated for pastes with 0.35 and 0.45 w/b. The rheological values measured using
242 the CCR protocol of pastes with nanoclays and different w/b ratio are summarized in Table
243 4. Pastes with 0.35 w/b exhibited higher peak values and equilibrium values than pastes with
244 0.45 w/b, except in the case of BE (0.63 and 0.8 for 0.35 w/b and 11.48 and 7.57 for 0.45
245 w/b, respectively). I_{thix} ranged from 0.76 to 3.91 and was higher at 0.45 w/b for all the pastes
246 with nanoclays, except ATT that remained constant at 1.02. Reference paste had slight
247 changes of I_{thix} between both w/b ratios. SEW was the paste that presented higher I_{thix} in
248 pastes with both 0.35 and 0.45 w/b. The characteristic time (T_{ch}), the time needed to reach
249 the steady state equilibrium value ranged from 34 to 276 s, showed to depend on w/b and
250 were higher for 0.35 w/b than for 0.45 w/b.

251 **3.3.2.2. Rate of reversible structural build-up (A_{thix})**

252 The rate of reversible structural build-up of a cement paste (A_{thix}) can be measured as the
253 linear increase of yield stress of the paste at rest during time, and can be calculated from CCR
254 protocol (Figure 7) according to (Eq. 3) [19, 23] :

$$A_{\text{thix}} = \frac{\tau_{pv-t} - \tau_{pv-0}}{T_{\text{rest}}} \quad (\text{Eq. 3})$$

where τ_{pv-0} is the peak value at initial time, τ_{pv-t} is the peak value at a specific resting time (T_{rest}). The rheological parameters measured to calculate A_{thix} of pastes with nanoclays and 0.35 w/b at 0 and 30 minutes resting times are summarized in Table 5.

The reference paste (REF) showed zero A_{thix} , as both peak yield stress at 0 and 30 minutes were 1.47 Pa. Nevertheless, the peak value raised from 0 to 30 minutes for all the pastes with nanoclays, producing A_{thix} ranging from 0.21 to 1.04. The highest values of A_{thix} were measured for pastes with sepiolite (1.04 for SEP and 0.87 for SEW), showing similar increments from 0 to 30 minutes (31.34 and 26.03 Pa, respectively). ATT and BE showed lower A_{thix} values (0.43 and 0.21 Pa, respectively).

4. Discussion

4.1 Influence of nanoclay type on cement paste flowability and rheological parameters

The experimental results pointed out that the type of nanoclay has a main effect on its influence on flowability and rheology of cement pastes. The different effect can be related to the particle size, shape and structural morphology differences of nanoclays [10, 25].

Cement paste with Attapulgite (ATT), a nanoclay that has a needle particle shape of short length, exhibited a flow behavior similar to the reference paste with limestone filler (REF). Its low water adsorption (Figure 2) did not affect the HRWRA efficiency (Figures 4 and 5). When compared to reference paste with the same flowability, ATT showed an increase of yield stress, I_{thix} and A_{thix} as expected [28-30], while viscosity remained very similar.

Pastes with sepiolite, a nanoclay with needle particle shape and larger length than ATT required larger amounts of HRWRA to reach flowability when w/b was low (0.35). In this case, the larger water adsorption of sepiolite due to probably to its higher BET surface area

278 (Figure 2), explain the reduction of HRWRA efficiency with this nanoclay particle. Both
279 sepiolites, dispersed (*Sew*) and in powder form (*Sep*), showed a similar flowability in pastes
280 with HRWRA (Figure 4), although *Sep* needed larger w/b in pastes without HRWRA (Figure
281 3). This different evolution of flowability could be due to an entanglement produced by
282 needle particle shape on samples with sepiolite in powder form [33]. That not happened with
283 *Sew* because of it is a functionalized component. Both sepiolites increased yield stress,
284 viscosity, I_{thix} and A_{thix} , with high values, larger than ATT. Although both are the same type
285 of clay, the larger particle size of sepiolites improved their effect on paste rheology [25, 26].
286 *Sew* produced the highest values of yield stress and increased I_{thix} due to its functionalization.
287 Bentonite (*Be*), which has a plate particle shape, showed a high demand of HRWRA to spread
288 with 0.35 w/b (Figure 4) due to its particle structural morphology and size [27, 36, 38, 39].
289 Moreover, cement paste with *Be* is clearly affected by the house-of-card network
290 microstructure that reduced the flowability of this pastes and is formed by this nanoclay [3,
291 35, 36]. The large amount of HRWRA required to get flowability reduced yield stress,
292 viscosity, I_{thix} and A_{thix} . Increasing w/b to 0.45 (Figure 5), improved HRWRA efficiency as
293 the nanoclay got saturated of water. Rheological parameters were also increased for BE and
294 0.45 w/b.

295 **4.2. Assessment of rheological properties on cement paste with nanoclays.**

296 Dynamic shear rheometer (DSR) results showed a non-linear behavior of pastes with
297 nanoclays (Figure 6). As described elsewhere, the modified Bingham model produced a
298 better adjustment than other models to calculate yield stress and viscosity, due to the effect
299 of nanoclays [14]. The increment of w/b reduced the rheological parameters, particularly
300 viscosity (Table 3). This reduction can be also identified by the final spread flow times

301 measured with the mini-cone (Figure 3 and Figure 5), due to the water saturation of nanoclays
302 in 0.45 w/b pastes. It must be highlighted that yield stress reduction was not as substantial as
303 viscosity.

304 Thixotropy Index (I_{thix}) was higher for pastes with 0.45 than those with 0.35 w/b.
305 Nevertheless, yield stress peak and equilibrium values of pastes with 0.45 w/b were
306 significantly lower than pastes with 0.35 w/b, but equilibrium values had a larger reduction.
307 The lower viscosity is behind this larger reduction of 0.45 w/b pastes. Therefore, I_{thix} is a
308 relative index that needs to be complemented with the reference peak value to fully
309 understand the instantaneous structural build-up of cement pastes.

310 When structural build-up was studied with A_{thix} (Roussel model), all peak values increased
311 over rest time, with the exception of the reference paste [19, 23]. Hence, all nanoclays showed
312 build-up capacity to modify the rheology of fluid cement pastes after a resting time [28-32].
313 Both sepiolites produced the highest A_{thix} value, although it was slightly higher for SEP,
314 probably due to the *SeW* functionalization. ATT produced lower A_{thix} than sepiolites possibly
315 due to its smaller particle length [25].

316 **4.3. Interactions of nanoclays with HRWRA and w/b: effects on paste flowability and** 317 **rheology**

318 The amount of HRWRA required to reach 330 ± 30 mm spread diameter in the mini-cone test
319 depended on the type of nanoclay and w/b. The effect on flowability and rheological
320 properties of pastes can be related to the interactions among nanoclays, HRWRA and water.
321 Water adsorption of Nanoclays showed to be affected by solution pH and cement pore
322 solution increased adsorptivity regarding tap water. The reduction of water available in the
323 fresh cement paste due to water adsorption of nanoclays produced a loss of flowability.

324 Above a certain w/b, nanoclays were saturated of water (*saturation threshold*) and all
325 nanoclays spread similarly (Figure 3).

326 The experimental results showed that only when this threshold was not reached (0.35 w/b),
327 interactions among nanoclays, water and HRWRA occurred [35, 36, 39]. These interactions
328 can be associated with clay particle size, shape and S_{BET} of nanoclays (Table 2.) [10, 25, 26,
329 38]. On one hand, Sepiolites had higher S_{BET} which corresponded to a higher water
330 adsorption. However, their needle particle shape produced lower water adsorption than
331 bentonite (*Be*), with plate particle shape, which demanded larger amounts of HRWRA in
332 order to change the flowability of pastes [27, 34, 39]. This negative interaction between *Be*
333 and HRWRA of paste with 0.35 w/b can also be appreciated on the lower values of BE for
334 structural build-up parameters (I_{thix} and A_{thix}) than those of sepiolites (Tables 4 and 5).

335 Another effect of this interactions is the increase of viscosity of the paste when HRWRA was
336 added, as the final spread flow time (Figure 3) only reached several seconds after the
337 incorporation of HRWRA on pastes (Figures 4 and 5). Hence, HRWRA was able to change
338 the spread mechanism of pastes related to viscosity, further than only increasing fluidity [4-
339 6]. However, final time values were slightly affected by nanoclays, as all pastes showed
340 similar times values at 330 ± 30 mm final spread diameter (Figures 4 and 5). The increase of
341 water in the paste (0.45 w/b) produced a shorter final time because less amount of HRWRA
342 was required to reach the target diameter [7]. Besides, It must be considered that mini-cone
343 slump test is a method with some limitations, although the results obtained in this paper with
344 mini-cone slump test were correlated with rheological parameters measured with DSR.

345 **5. Conclusions**

346 This paper presents a study on cement-limestone filler blended SCC pastes with 2 % of four
347 types of nanoclays: attapulgite, bentonite and sepiolite in powder form and dispersed in water.
348 Their effect on flowability and rheology parameters of the pastes was evaluated. Two water
349 to binder ratios (0.35 and 0.45 w/b) were used and a high range water reducing admixture
350 (HRWRA) was incorporated to reach a target flowability of 330 ± 30 mm in a mini-cone test.

351 The main conclusions of the study were:

- 352 • The pH of the water solution influenced nanoclays water adsorption regardless the
353 nanoclay type. The alkaline pH of cement pore solution increased substantially
354 adsorption nanoclays water adsorption.
- 355 • Water adsorption of nanoclays is related to their particle size and shape. The needle
356 particle shape with large particles of Sepiolite in powder form reduced drastically
357 paste flowability. The introduction of a HRWRA in the paste minimized this effect.
358 Sepiolite dispersed in water did not show this problem due to its functionalized
359 particles.
- 360 • The water adsorbed by nanoclays reduced the water available in the paste, reducing
361 paste flowability, especially for low w/b (0.35). Overpassing an adsorption threshold
362 with a higher w/b (0.45) minimized this undesirable effect and increased HRWRA
363 effectiveness.
- 364 • The incorporation of a HRWRA in pastes with nanoclays modified both yield stress
365 and viscosity.

- 366 • Paste with bentonite and 0.45 w/b required the same percentage of HRWRA to reach
367 large flowability than all other nanoclays due to the *saturation threshold* of this
368 nanoclay was overpassed and HRWRA worked effectively.
- 369 • All nanoclays used in this study modified the rheological properties on fluid cement
370 pastes, particularly sepiolites reached the higher values of yield stress and viscosity..
371 The increment of water produced a reduction of viscosity in all nanoclays. Thus, peak
372 value and steady-state value were lower with 0.45 w/b and thixotropy index (I_{thix}) was
373 higher than pastes with 0.35 w/b. Moreover, resting time increased yield stress (peak
374 values) with nanoclays and improved the rate of reversible structural build-up (A_{thix}).

375 **Acknowledgements**

376 The authors would like to acknowledge the financial support of the Spanish Ministry of
377 Economy and Competitiveness as part of the project NanoCompaC (BIA2016-77911-R) and
378 the technical support of the companies TOLSA GROUP S.A, BASF construction chemicals,
379 Omya Clariana and Cementos Portland Valderrivas, SA.

380 **References**

- 381 [1] G. Barluenga, M. Giménez, A. Rodríguez, O. Rio, Quality control parameters for
382 on-site evaluation of pumped self-compacting concrete, *Constr. Build. Mater.* 154
383 (2017) 1112-1120, <https://doi.org/10.1016/j.conbuildmat.2017.07.223>.
- 384 [2] G.R. Lomboy, X. Wang, K. Wang, Rheological behavior and formwork pressure of
385 SCC, SFSCC, and NC mixtures, *Cem. Concr. Compos.* 54 (2014) 110-116,
386 <https://doi.org/10.1016/j.cemconcomp.2014.05.001>
- 387 [3] Y. Qian, G. De Schutter, Enhancing thixotropy of fresh cement pastes with nanoclay
388 in presence of polycarboxylate ether superplasticizer (PCE), *Cem. Concr. Res.*, 111
389 (2018) 15-22, <https://doi.org/10.1016/j.cemconres.2018.06.013>
- 390 [4] N. Roussel, P. Coussot, Fifty-cent rheometer for yield stress measurements: From
391 slump to spreading flow. *J. Rheol.* 49 (2005) 705-718. DOI.10.1122/1.1879041g
- 392 [5] N. Roussel, C. Stefani, R. Leroy, From mini-cone test to Abrams cone test:
393 measurement of cement-based materials yield stress using slump tests, *Cem. Concr.*
394 *Res.* 35:5 (2005) 817-822, <https://doi.org/10.1016/j.cemconres.2004.07.032>
- 395 [6] N. Tregger, L. Ferrara, S.P Shah, Identifying viscosity of cement paste from mini-
396 slump-flow test. *ACI Mater. J.* 105:6 (2008) 558-566, [https://doi.org/10.3141/2141-](https://doi.org/10.3141/2141-12)
397 12.
- 398 [7] L. Ferrara, M. Cremonesi, N. Tregger, A. Frangi, S. P. Shah, On the identification of
399 rheological properties of cement suspensions: Rheometry, Computational Fluid
400 Dynamics modeling and field test measurements, *Cem. Concr. Res.* 42 (2012) 1134-
401 1146, <https://doi.org/10.1016/j.cemconres.2012.05.007>.
- 402 [8] M.S. Choi, J.S. Lee, K.S. Ryu, K.T. Koh, S.H. Kwon, Estimation of rheological
403 properties of UHPC using mini slump test, *Constr. Build. Mater.* 106 (2016) 632-
404 639, <https://doi.org/10.1016/j.conbuildmat.2015.12.106>.

- 405 [9] A. Bouvet, E. Ghorbel, R. Bennacer, The mini-conical slump flow test: Analysis and
406 numerical study, *Cem. Concr. Res.* 40 :10, (2010) 1517-1523,
407 <https://doi.org/10.1016/j.cemconres.2010.06.005>.
- 408 [10] M. Jalal, E. Teimortashlu, Z. Grasley, Performance-based design and
409 optimization of rheological and strength properties of self-compacting cement
410 composite incorporating micro/nano admixtures, *Compos. B Eng.* 163 (2019) 497-
411 510, <https://doi.org/10.1016/j.compositesb.2019.01.028>.
- 412 [11] J. J. Assaad, J. S. Harb, Y. Maalouf, Effect of vane configuration on yield
413 stress measurements of cement pastes, *J non-newton fluid.*, 230 (2016) 31-42,
414 <https://doi.org/10.1016/j.jnnfm.2016.01.002>.
- 415 [12] D. Feys, R. Cepuritis, S. Jacobsen, K. Lesage, E. Secrieru, A. Yahia,
416 Measuring rheological properties of cement pastes: most common techniques,
417 procedures and challenges, *RILEM Tech. Lett.* 2 (2017) 129-135,
418 [dx.doi.org/10.21809/rilemtechlett.2017.43](https://doi.org/10.21809/rilemtechlett.2017.43).
- 419 [13] Q. Yuan, D. Zhou, K. H. Khayat, D. Feys, C. Shi, On the measurement of
420 evolution of structural build-up of cement paste with time by static yield stress test
421 vs. small amplitude oscillatory shear test, *Cem. Concr. Res.* 99 (2017) 183-189,
422 <https://doi.org/10.1016/j.cemconres.2017.05.014>.
- 423 [14] D. Feys, J. E. Wallevik, A. Yahia, K. H. Khayat, O. H. Wallevik, Extension of
424 the Reiner–Riwlin equation to determine modified Bingham parameters measured in
425 coaxial cylinders rheometers, *Mater. Struct.* 46 (2013) 289–311, DOI
426 10.1617/s11527-012-9902-6.
- 427 [15] K. H. Khayat, J. J. Assaad, Use of thixotropy-enhancing agent to reduce
428 formwork pressure exerted by self-consolidating concrete, *ACI Mater. J.*, 105 (2008)
429 88-96, doi?
- 430 [16] J. J. Assaad, Correlating water extraction to viscosity variations of injection
431 grouts, *Constr. Build. Mater.* 77 (2015) 74-
432 82, <https://doi.org/10.1016/j.conbuildmat.2014.12.024>.
- 433 [17] M. Tuyan, R. S. Ahari, T. K. Erdem, Ö. A. Çakır, K. Ramyar Influence of
434 thixotropy determined by different test methods on formwork pressure of self-
435 consolidating concrete, *Constr. Build. Mater.* 173 (2018) 189-200,
436 <https://doi.org/10.1016/j.conbuildmat.2018.04.046>.

- 437 [18] J. T. Kolawole, R. Combrinck, W. P. Boshoff, Measuring the thixotropy of
438 conventional concrete: The influence of viscosity modifying agent, superplasticiser
439 and water, *Constr. Build. Mater.* 225 (2019) 853-867,
440 <https://doi.org/10.1016/j.conbuildmat.2019.07.240>.
- 441 [19] N. Roussel, A thixotropy model for fresh fluid concretes: Theory, validation
442 and applications, *Cem. Concr. Res.*, 36 (2006) 1797-1806,
443 <https://doi.org/10.1016/j.cemconres.2006.05.025>.
- 444 [20] R. Ferron, A. Gregori, Z. Sun, S. P. Shah, Rheological Method to Evaluate
445 Structural Build-Up in Self- Consolidating Concrete Cement Paste, *ACI Mater. J.*
446 104:3 (2007) 242-250. DOI.10.14359-18669.
- 447 [21] T. Lecompte, A. Perrot, Non-linear modeling of yield stress increase due to
448 SCC structural build-up at rest, *Cem. Concr. Res.* 92 (2017) 92-97,
449 <https://doi.org/10.1016/j.cemconres.2016.11.020>.
- 450 [22] D. Lowke, Thixotropy of SCC—A model describing the effect of particle
451 packing and superplasticizer adsorption on thixotropic structural build-up of the
452 mortar phase based on interparticle interactions, *Cem. Concr. Res.* 104 (2018) 94-
453 104, <https://doi.org/10.1016/j.cemconres.2017.11.004>.
- 454 [23] A. Perrot, T. Lecompte, P. Estellé, S. Amziane, Structural build-up of rigid
455 fiber reinforced cement-based materials, *Mater. Struct.* 46 (2013) 1561–1568,
456 <https://doi.org/10.1617/s11527-012-9997-9>.
- 457 [24] Y. Qian, K. Lesage, K. El Cheikh, G. De Schutter, Effect of polycarboxylate
458 ether superplasticizer (PCE) on dynamic yield stress, thixotropy and flocculation
459 state of fresh cement pastes in consideration of the Critical Micelle Concentration
460 (CMC), *Cem. Concr. Res.* 107 (2018) 75-84,
461 <https://doi.org/10.1016/j.cemconres.2018.02.019>.
- 462 [25] H. H. Murray, Structure and Composition of the Clay Minerals and their
463 Physical and Chemical Properties, in: Elsevier (Eds.), applied clay mineralogy
464 occurrences, processing and application of kaolins, bentonites, palygorskite-
465 sepiolite, and common clays, Amsterdam, The Netherlands, 2007, pp. 7-31.
- 466 [26] A. Álvarez, J. Santarén, A. Esteban-Cubillo and P. Aparicio, Current
467 Industrial Applications of Palygorskite and Sepiolite, in: Elsevier (Eds.),
468 Developments in Palygorskite-Sepiolite Research: a new outlook on these

- 469 nanomaterials, Amsterdam, The Netherlands, 2011, pp. 281-298,
470 <https://doi.org/10.1016/B978-0-444-53607-5.00012-8>.
- 471 [27] M.L. Nehdi, Clay in cement-based materials: Critical overview of state-of-
472 the-art, *Constr. Build. Mater.* 51 (2014) 372-382,
473 <https://doi.org/10.1016/j.conbuildmat.2013.10.059>.
- 474 [28] N.A. Tregger, M. E. Pakula, S. P. Shah, Influence of clays on the rheology of
475 cement pastes, *Cem. Concr. Res.* 40 (2010) 384-391,
476 <https://doi.org/10.1016/j.cemconres.2009.11.001>
- 477 [29] S. Kawashima, M. Chaouche, D. J. Corr, S. P. Shah, Rate of thixotropic
478 rebuilding of cement pastes modified with highly purified attapulgite clays, *Cem.*
479 *Concr. Res.* 53 (2013) 112-118, <https://doi.org/10.1016/j.cemconres.2013.05.019>.
- 480 [30] S. Kawashima, P. Hou, D. J. Corr, S. P. Shah, Modification of cement-based
481 materials with nanoparticles, *Cem. Concr. Compos.* 36 (2013) 8-15.
482 <https://doi.org/10.1016/j.cemconcomp.2012.06.012>.
- 483 [31] Q. Yuan, D. Zhou, B. Li, H. Huang, C. Shi, Effect of mineral admixtures on
484 the structural build-up of cement paste, *Constr. Build. Mater.* 160 (2018) 117-126,
485 <https://doi.org/10.1016/j.conbuildmat.2017.11.050>.
- 486 [32] Z. Quanji, G.R. Lomboy, K. Wang, Influence of nano-sized highly purified
487 magnesium alumino silicate clay on thixotropic behavior of fresh cement pastes,
488 *Constr. Build. Mater.* 69 (2014) 295-300,
489 <https://doi.org/10.1016/j.conbuildmat.2014.07.050>
- 490 [33] R. D. Ferron, S. P. Shah, E. Fuente, C. Negro, Aggregation and breakage
491 kinetics of fresh cement paste, *Cem. Concr. Res.* 50 (2013) 1-10,
492 <https://doi.org/10.1016/j.cemconres.2013.03.002>.
- 493 [34] A. Kaci, M. Chaouche, P-A. Andréani, Influence of bentonite clay on the
494 rheological behaviour of fresh mortars, *Cem. Concr. Res.* 41 (2011) 373-379,
495 <https://doi.org/10.1016/j.cemconres.2011.01.002>
- 496 [35] I. Dejaeghere, M. Sonebi, G. De Schutter, Influence of nano-clay on rheology,
497 fresh properties, heat of hydration and strength of cement-based mortars, *Constr.*
498 *Build. Mater.* 222 (2019) 73-85. <https://doi.org/10.1016/j.conbuildmat.2019.06.111>.
- 499 [36] L. Lei, J. Plank, A study on the impact of different clay minerals on the
500 dispersing force of conventional and modified vinyl ether based polycarboxylate

501 superplasticizers, *Cem. Concr. Res.* 60 (2014) 1-10,
502 <https://doi.org/10.1016/j.cemconres.2014.02.009>.

503 [37] Mechtcherine, E. Secieru, C. Schröfl, Effect of superabsorbent polymers
504 (SAPs) on rheological properties of fresh cement-based mortars – Development of
505 yield stress and plastic viscosity over time, *Cem. Concr. Res.* 67 (2015) 52-65,
506 <https://doi.org/10.1016/j.cemconres.2014.07.003>

507 [38] H. Tan, C. Qi, B. Ma, X. Li and S. Jian, Effect of polycarboxylate
508 superplasticiser adsorption on fluidity of cement–clay system, *Mater. Res. Innov.* 19
509 (2015) 423-428, <https://doi.org/10.1179/1432891714Z.0000000001124>.

510 [39] S. Ng, J. Plank, Interaction mechanisms between Na-montmorillonite clay
511 and MPEG-based polycarboxylate superplasticizers, *Cem. Concr. Res.* 42 (2012)
512 847-854, <https://doi.org/10.1016/j.cemconres.2012.03.005>.

513

514

515 **List of Tables:**

516 **Table 1.** Cement pastes' compositions

517 **Table 2.** Nanoclays' properties.

518 **Table 3.** Rheological properties of pastes with Nanoclays (measured using DSR with CS
519 protocol).

520 **Table 4.** Rheological properties of pastes with nanoclays calculated using DSR with CCR
521 protocol (IThix calculated according to Qian model [3, 24]).

522 **Table 5.** Rheological properties of pastes with nanoclays calculated using DSR with CCR
523 protocol. (AThix was calculated according to Roussel model [19, 23]).

524

525 **List of Figures:**

526 **Figure 1.** –DSR protocols: CS, Shear stress control; CCR, Shear rate control.

527 **Figure 2.** Figure 2 – Water Adsorption values over time of nanoclays. a) water adsorption
528 on alkaline water (cement pore solution); b) water adsorption on tap water.

529 **Figure 3.** Mini-cone slump test of pastes with different w/b. a) Final spread diameter; b)
530 Final spread time values.

531 **Figure 4.** Mini-cone slump test of pastes with nanoclays and HRWRA (w/b - 0.35). a)
532 Final spread diameter; b) Final spread time

533 **Figure 5.** Mini-cone slump test of pastes with nanoclays and HRWRA (w/b - 0.45). a)
534 Final spread diameter; b) Final spread time.

535 **Figure 6.** DSR results of CS protocol. a) Shear stress vs rate for 0.35w/b; b) Shear stress vs
536 rate for 0.45w/b.

537 **Figure 7.** DSR results of CCR protocol. a) Shear stress vs time with w/b of 0.35 and 0min;
538 b) Shear stress vs time with w/b of 0.45 and 0min; c) Shear stress vs time with
539 w/b of 0.35 and 30min;

540

541 **Table 1. Cement pastes' compositions**

	REF	ATT	BE	SEP	SEW	REF	ATT	BE	SEP	SEW
cement	850	850	850	850	850	850	850	850	850	850
Filler	425	425	425	425	425	425	425	425	425	425
Water *	446	446	446	446	386	574	574	574	574	514
HRWRA **	0 - 2%					0 - 1%				
ATT	-	17	-	-	-	-	17	-	-	-
BE	-	-	17	-	-	-	-	17	-	-
SEP	-	-	-	17	-	-	-	-	17	-
SEW ***	-	-	-	-	17*	-	-	-	-	17*
w/b****	0.35	0.35	0.35	0.35	0.35	0.45	0.45	0.45	0.45	0.45

* Liquid water added.

** HRWRA was employed as an increment dosage scale, by cement weight.

*** Solid residue 22%.

**** Water of the components (HRWRA and SEW) was also taken into account.

542

543

544 **Table 2. Nanoclays' properties.**

Component	S _{bet} (m ² /g)	D[4,3] (μm)
Attapulgite (<i>Att</i>)	144	21,97
Bentonite (<i>Be</i>)	138	38.42
Sepiolite (<i>Sep</i>)	316	39.66
Sepiolite* (<i>Sew</i>)	284	57.7

* Dispersed in water.

545

546

547 **Table 3. Rheological properties of pastes with Nanoclays (measured using DSR with CS**
548 **protocol).**

w/b	Sample	yield stress (Pa)	viscosity (Pa·s)
0.35	REF	8.3	0.57
	ATT	23.9	0.46
	BE	10.0	0.29
	SEP	28.9	0.65
	SEW	94.8	0.95
0.45	REF	10.6	0.06
	ATT	15.9	0.17
	BE	29.2	0.21
	SEP	24.8	0.22
	SEW	48.2	0.34

549

550

551 **Table 4. Rheological properties of pastes with nanoclays calculated using DSR with**
 552 **CCR protocol (I_{Thix} calculated according to Qian model [3, 24]).**

w/b	Sample	τ_i (Pa)	τ_{eq} (Pa)	$\tau_i - \tau_{eq}$ (Pa)	T_{ch} (s)	$T_i - T_{eq}$ (s)	I_{Thix}
0.35	REF	1.47	1.93	-0.46	214	162	0.76
	ATT	9.68	9.46	0.22	84	50	1.02
	BE	0.63	0.8	-0.17	172	134	0.79
	SEP	32.9	27.65	5.25	240	224	1.19
	SEW	76.67	37.6	39.07	276	272	2.04
0.45	REF	1.26	1.3	-0.04	34	-0.04	0.97
	ATT	3.4	3.33	0.07	54	0.07	1.02
	BE	11.48	7.57	3.91	102	3.91	1.52
	SEP	9.695	6.47	3.23	136	3.23	1.50
	SEW	39.57	10.13	29.44	240	29.44	3.91

553

554

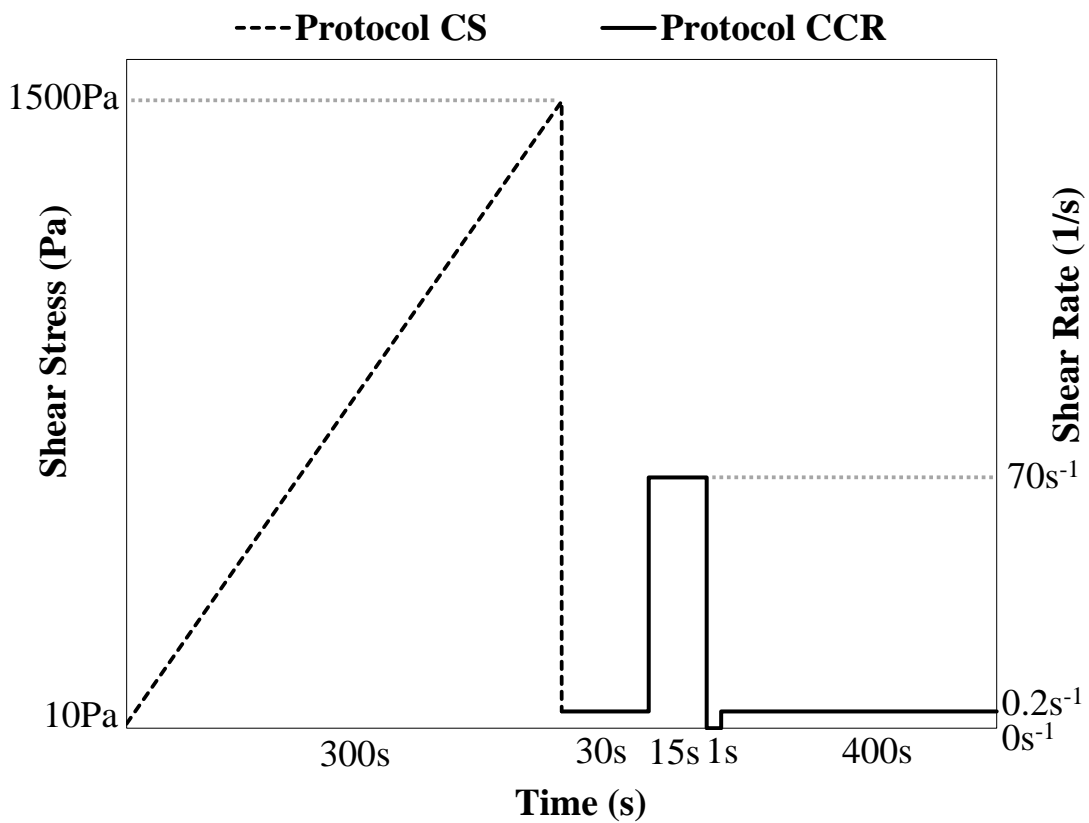
555 **Table 5. Rheological properties of pastes with nanoclays calculated using DSR with**
 556 **CCR protocol. (A_{Thix} was calculated according to Roussel model [19, 23]).**

w/b	Sample	τ_{pv-0} (Pa)	τ_{pv-30} (Pa)	$\tau_{pv-30} - \tau_{pv-0}$ (Pa)	T_{Rest} (min)	A_{Thix} (Pa/min)
0.35	REF	1.47	1.47	0	30	0.00
	ATT	9.68	22.66	12.98	30	0.43
	BE	0.63	6.848	6.22	30	0.21
	SEP	32.9	64.24	31.34	30	1.04
	SEW	76.67	102.7	26.03	30	0.87

557

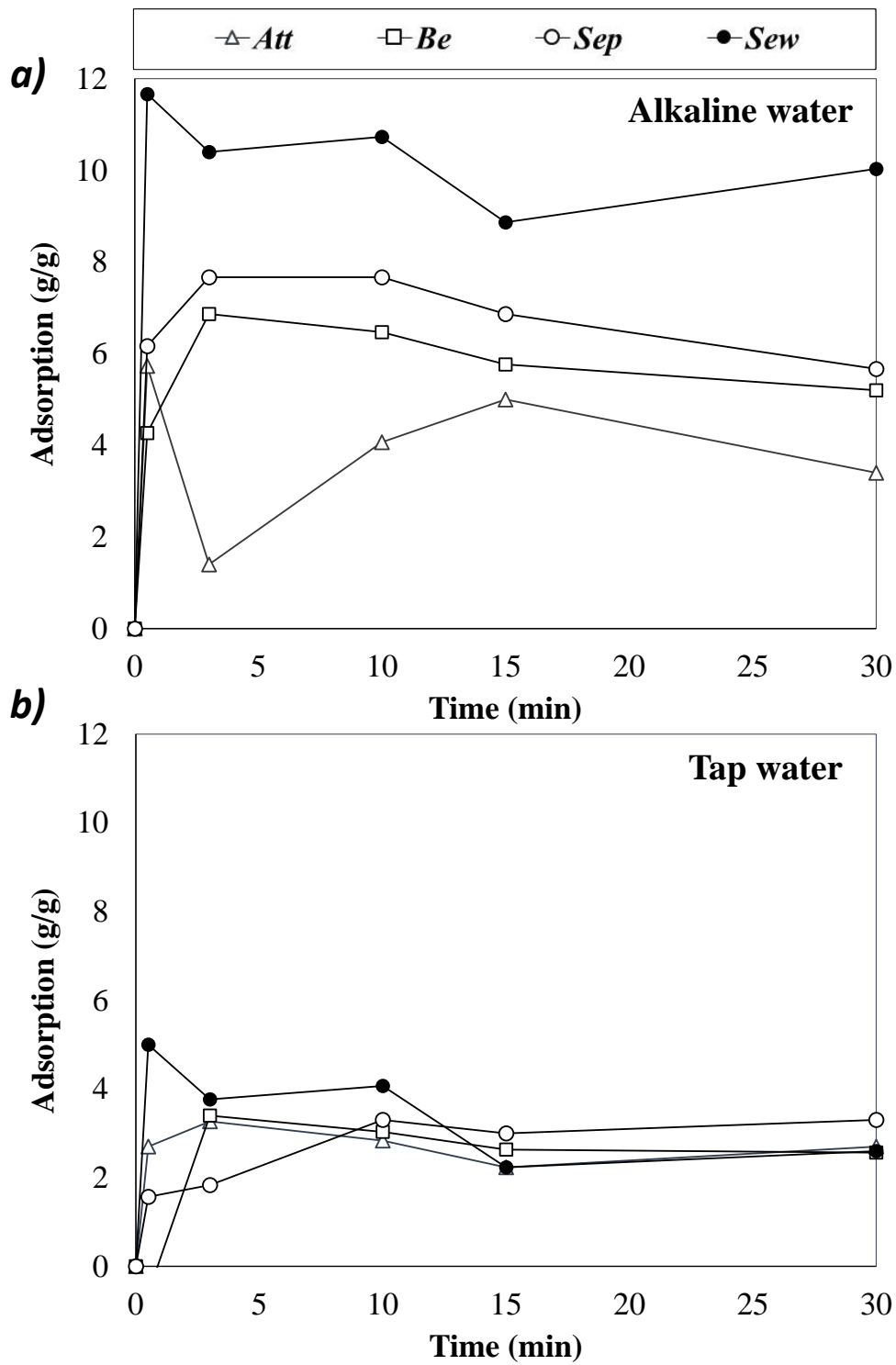
558

559 **Figure 1** – DSR protocols: CS, Shear stress control; CCR, Shear rate control.



560

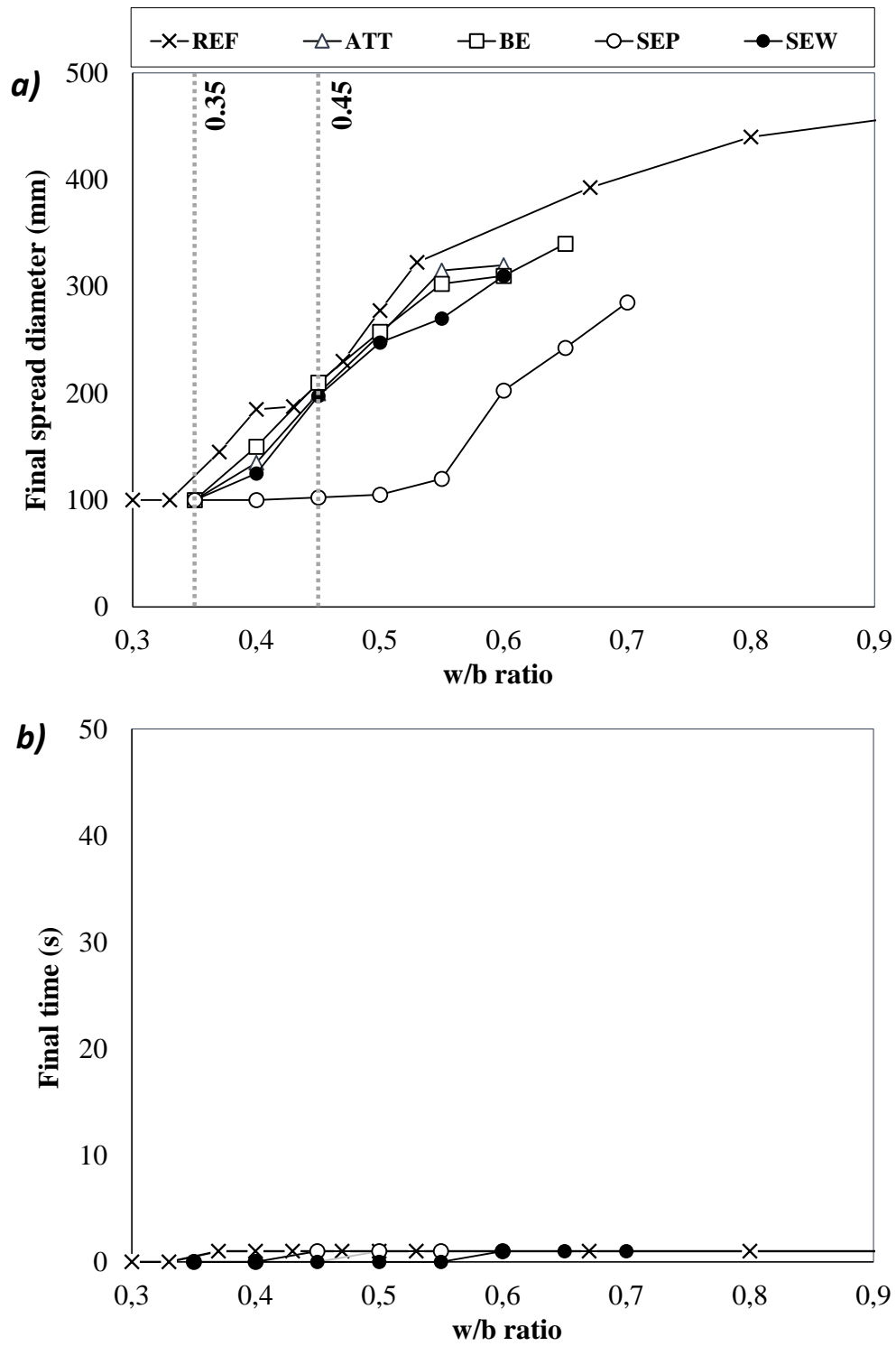
561 **Figure 2** – Water Adsorption values over time of nanoclays. a) water adsorption on alkaline
 562 water (cement pore solution); b) water adsorption on tap water.
 563



564
 565

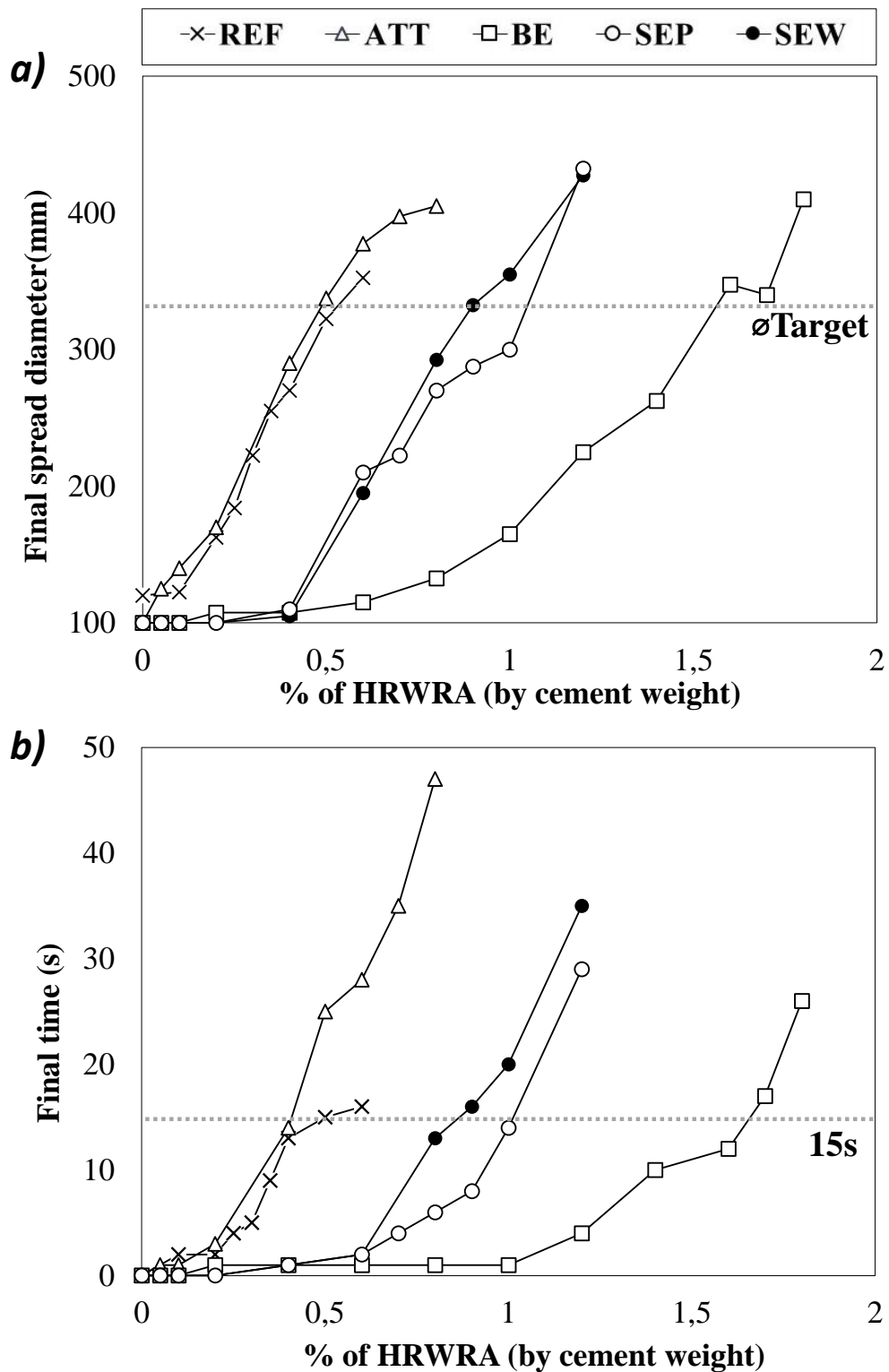
566
567
568
569

Figure 3 – Mini-cone slump test of pastes with different w/b. a) Final spread diameter; b) Final spread time values.



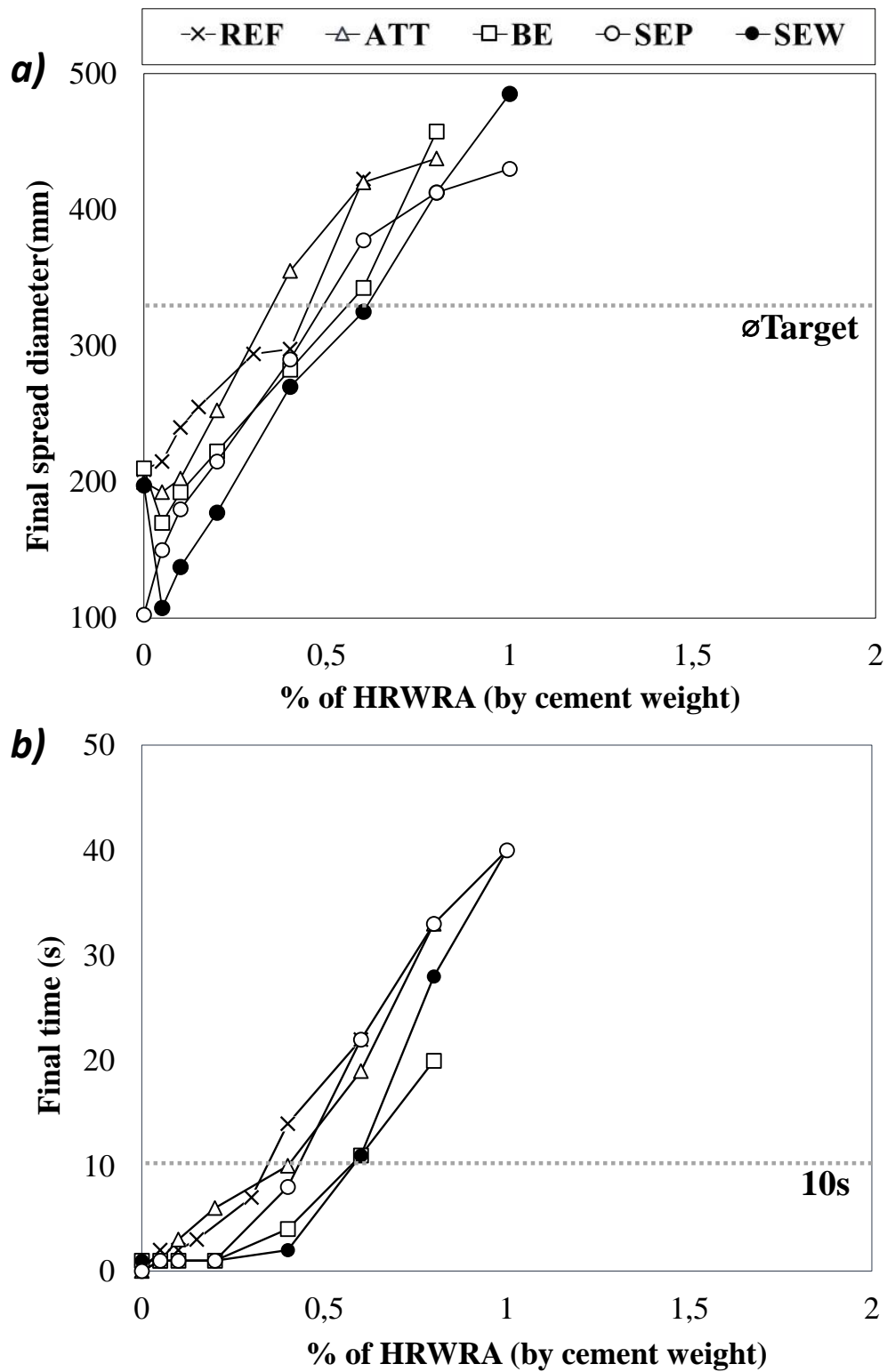
570
571

572 **Figure 4.** Mini-cone slump test of pastes with nanoclays and HRWRA (w/b - 0.35). a) Final
 573 spread diameter; b) Final spread time
 574



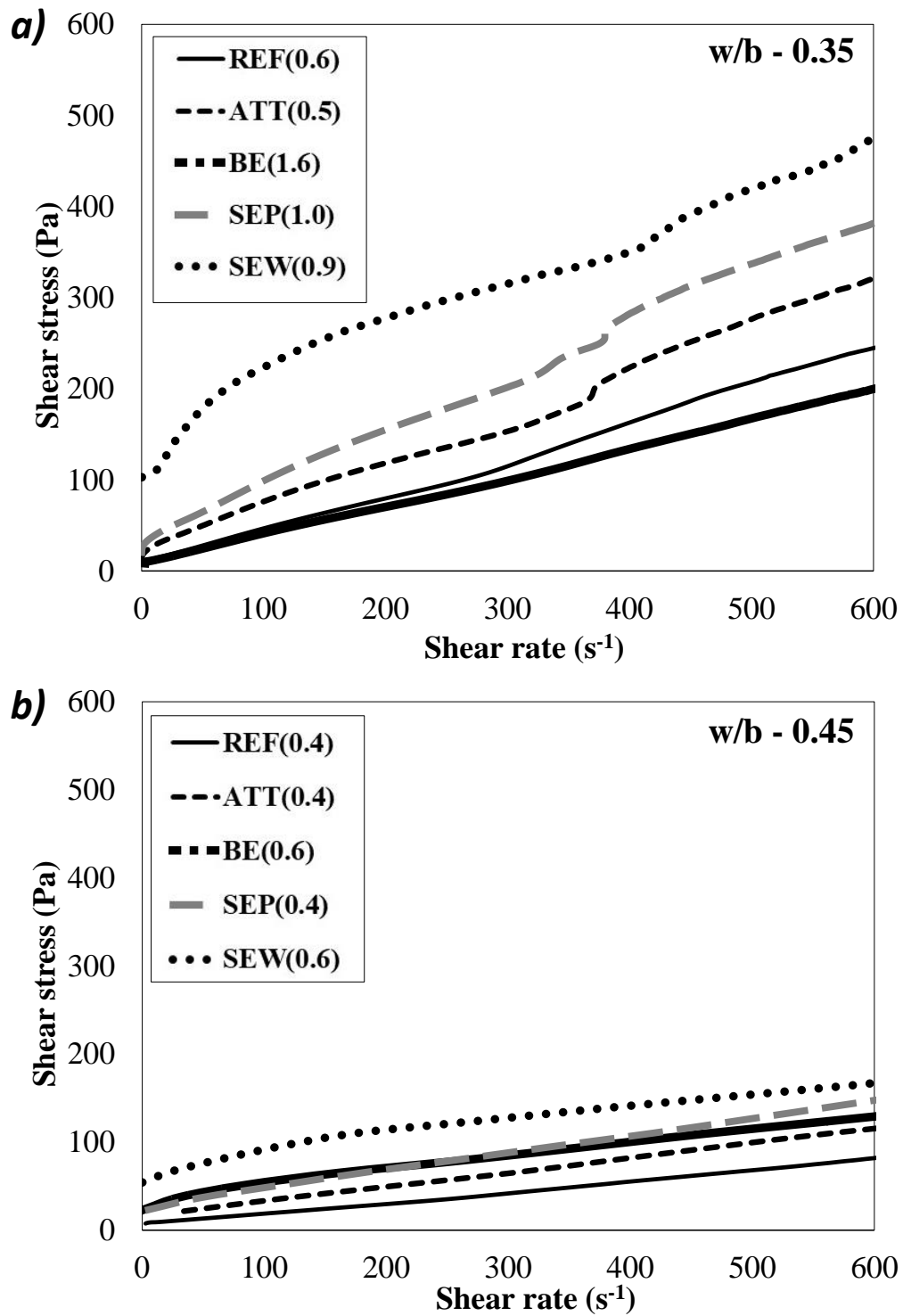
575

576 **Figure 5.** Mini-cone slump test of pastes with nanoclays and HRWRA (w/b - 0.45). a) Final
 577 spread diameter; b) Final spread time.
 578



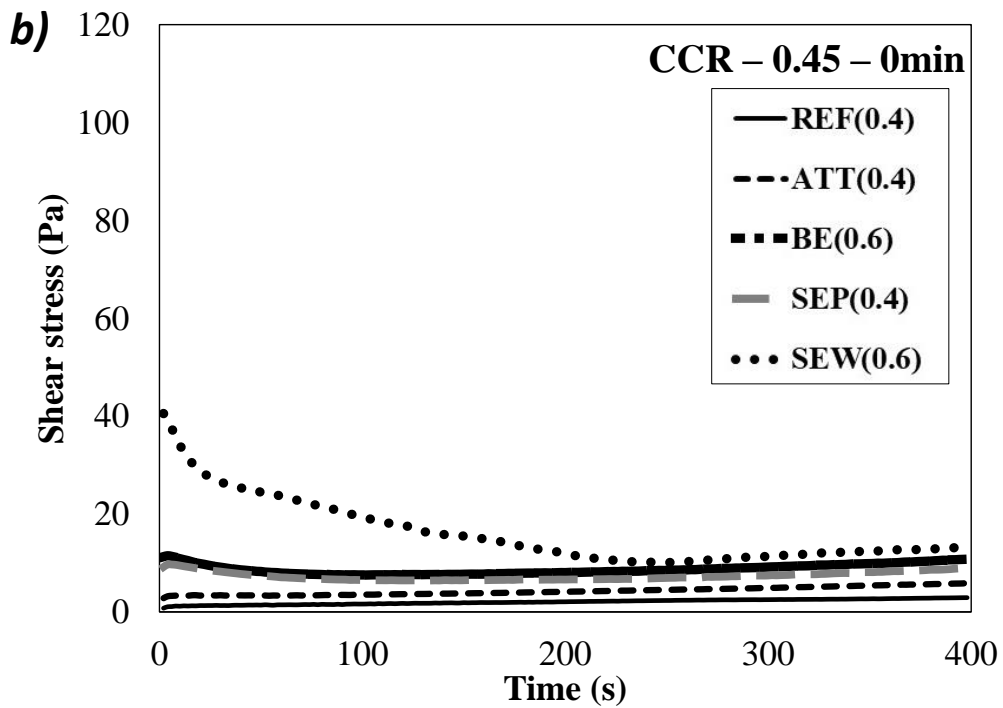
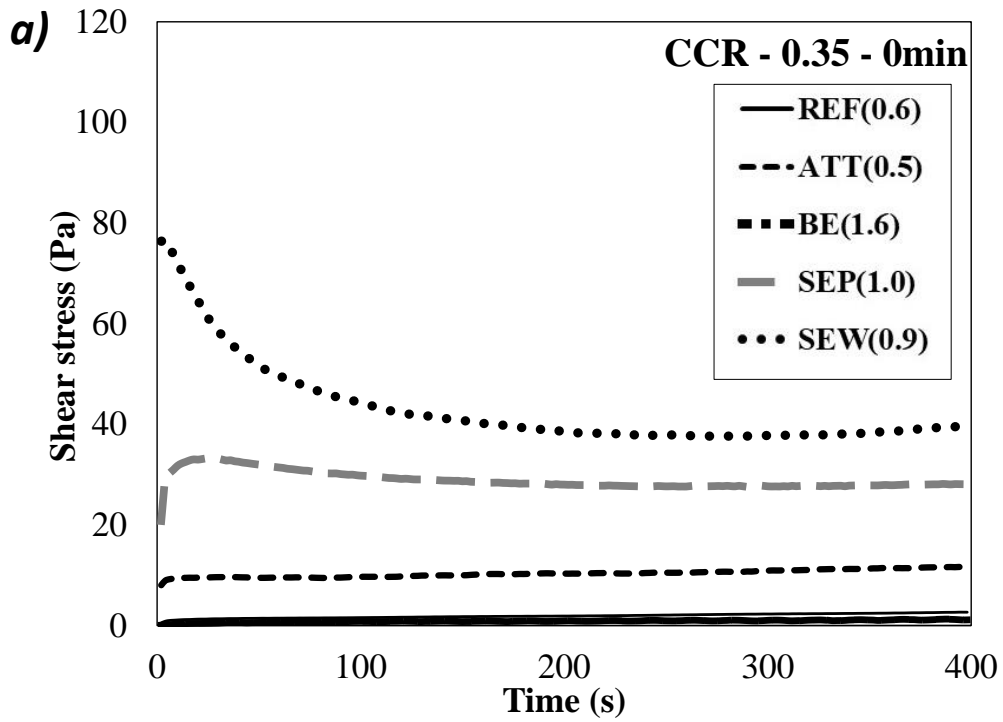
579

580 **Figure 6** – DSR results of CS protocol. a) Shear stress vs rate for 0.35w/b; b) Shear stress vs
 581 rate for 0.45w/b. (In brackets the amount of HRWRA)
 582

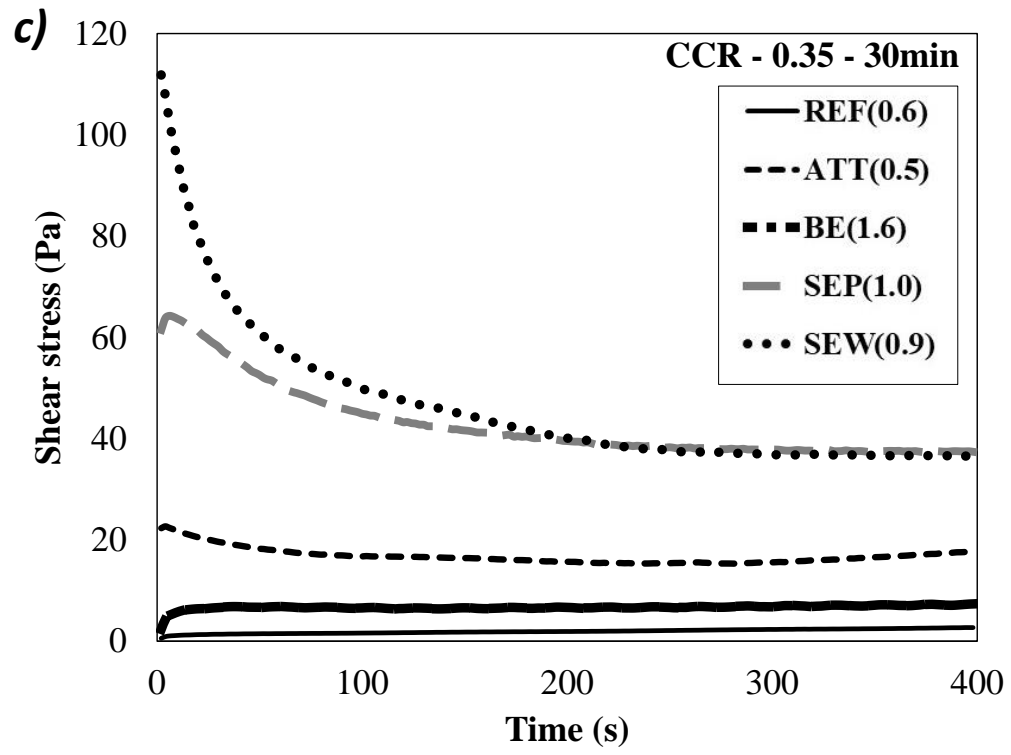


583

584 **Figure 7** – DSR results of CCR protocol. a) Shear stress vs time with w/b of 0.35 and 0min;
 585 b) Shear stress vs time with w/b of 0.45 and 0min; c) Shear stress vs time with w/b of 0.35
 586 and 30min. (In brackets the amount of HRWRA)



587
588



589